Pergamon

Int. J. Solids Structures Vol. 33, No. 1, pp. 1–10, 1996

0020-7683/96 $9.50 + .00

0020-7683(95)00025-9

AUTOMATED YIELD-LINE ANALYSIS OF ORTHOTROPIC SLABS

DAVID JOHNSON
Department of Civil and Structural Engineering, The Nottingham Trent University, Burton Street, Nottingham NG1 4BU, U.K.

(*Received* 11 *October* 1994; *in revised form* 28 *December* 1994)

Abstract— The rigid-plastic yield-line analysis of orthotropically reinforced concrete slabs under uniformly distributed loading is developed as the lower-bound form of a linear programming formulation. The analysis is extended to consider geometric variation of chosen yield-line patterns by the technique of sequential linear programming. It is shown that the omission, within the iterations of the sequential linear programming process, of the effects of geometric variation on yield-line ultimate moments of resistance leads to a formulation which is, at best, inefficient, and can be divergent or converge to an erroneous solution. Accordingly, a formulation is developed which includes a linearized representation of the geometric sensitivities of the resistance moments within the iteration process. This formulation is shown to be both effective and efficient for the yield-line analysis of a number of example slabs which include a range of support conditions and boundary geometries.

INTRODUCTION

Background

The author has previously investigated (Johnson, 1995) the yield-line analysis of isotropic slabs by using the technique of sequential linear programming. This method employs triangulated slab meshing to provide a system of edge lines, the moments along which are bounded by specified yield values. At the nodes of the meshing, linear constraints are developed which represent the equilibrium conditions between the slab loading (presumed uniform) and the edge moments. Subject to these equilibrium and yield constraints, the load factor is maximized by the use of linear programming to obtain the ultimate load and collapse mode. The geometry of the collapse mode may then be optimized by creating linearized approximations to represent the effects of variation in the mesh nodal coordinates on the equilibrium conditions. Repeated linear programming solutions are undertaken which provide a sequence of load factor sensitivities to geometric variation and allow the load factor to be minimized with respect to yield-line geometry.

Since the technique can only create yield-line systems from the edges of the meshing adopted, it is essential that the meshing is able to represent the critical collapse mode for the slab. Should the mode not be known *ab initio*, it has been recommended [see Johnson (1994a)], that a fine finite element mesh be adopted initially to give an indication of the critical mode. Subsequently, a simplified mesh is created to represent the critical mode and to form the basis for geometric variation investigations.

It has also proved possible to extend the formulation to the yield-line analysis of beam-slab systems [see Johnson (1994b)]. The present objective is to develop the technique further by considering the analysis of orthotropically reinforced slabs.

Representation of orthotropy

It is assumed that an orthotropic reinforcement layout is capable of providing yield moment vectors of magnitude m_u and m_v (Fig. 1). If the yield-line in Fig. 1 is inclined to the u-moment vector at an angle α and the u-direction is itself inclined to the reference x-direction at an angle ϕ, then, by the Johansen yield criterion, the magnitude of the moment vector in the direction of the yield line is given by:

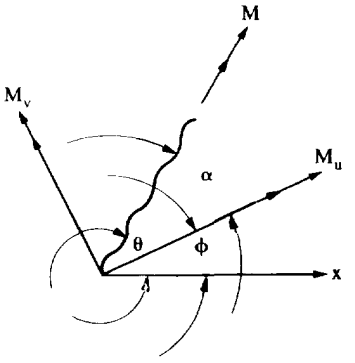

Fig. 1. Orthotropic moment vectors.

$$m = m_u \cos^2 \alpha + m_v \sin^2 \alpha. \tag{1}$$

If an automated yield-line analysis of an orthotropic slab is required, the yield-moments along the meshing lines must therefore be established from eqn (1), otherwise the procedure developed previously remains unchanged, unless optimization of the yield-line geometry is needed. If this is the case, then the orientations θ of the mesh lines will alter during the optimization process and, hence, the yield moments along the mesh lines will also change. Perhaps the most straightforward way of dealing with this feature is to assume that the effects of yield moment alteration are relatively minor, in comparison with the effects of geometric alteration on the equilibrium conditions. If this is so, then it is reasonable to ignore yield moment changes during the course of any particular geometric iteration and only evaluate the modified yield moments once a changed geometry has been established.

To investigate the performance of such a formulation, the simple example shown in Fig. 2(a) is considered. Making use of symmetry, the quarter slab shown in Fig. 2(b) was considered, using the triangular mesh indicated and allowing geometric variation in the horizontal (x) position of node 3 only. The variation in the collapse uniform load, q_u, with geometric iteration is indicated by the dashed line in Fig. 2(c), where it is compared with a

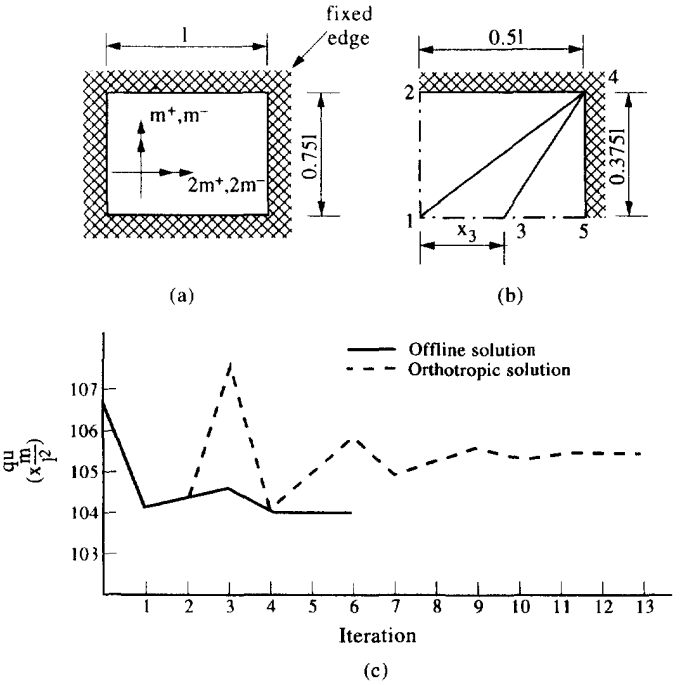

Fig. 2. (a) Fixed edge orthotropic rectangular slab. (b) Mesh for quarter slab. (c) Solution graph for affine and orthotropic solutions.

solution generated by consideration of the corresponding isotropic affine [see Wood (1961)] slab. The affine solution of $\ddot{q}_u = 104(m/l^2)$ and $\ddot{x}_3 = 0.16l$ (where $\ddot{}$ indicate a converged value) agrees closely with the closed form solution which may be readily obtained for this straightforward example. The orthotropic solution, however, although following the affine solution for the first two iterations, then diverges and eventually "converges" to an erroneous solution of $\ddot{q}_u = 105.5(m/l^2)$ and $\ddot{x}_3 = 0.08l$.

It may be noted that although the affine and orthotropic solutions vary widely in respect of the converged geometry (x_3) values, the converged values of collapse load differ by only 1.5%. This may be partly a reflection of the fact that convergence is based solely on collapse load variation, being presumed if the collapse load values of the three previous iterations vary by no more than 0.1%. It is also, no doubt, a reflection of a general property of collapse loads being relatively insensitive to geometric yield-line variation in the neighbourhood of the critical collapse mode geometry, especially in regions of positive (sagging) bending. If collapse loads alone are of significance, then it may be acceptable to use the simple treatment of orthotropy adopted above. In general, however, it may be concluded that it is not satisfactory to consider the effects of geometrical change on yield moment values separately from consideration of the effects of geometrical variation on the equilibrium conditions. It is therefore necessary to develop an appropriate theoretical model which incorporates simultaneous consideration of the effects of geometrical changes and such a model is developed in the next section.

YIELD-LINE ANALYSIS BY SEQUENTIAL LINEAR PROGRAMMING

Isotropic slabs without geometric optimization

It has been shown previously [see Johnson (1994a)] that if the slab triangulation is such that there are *nj* nodes at which normal displacement is allowed and *nb* moment-resisting boundaries, then summing contributions from all the *ne* triangular regions provides a set of equilibrium conditions, between the moments along the *nb* boundaries and the applied normal loads at the *nj* nodes, of the form:

$$\mathbf{C}\mathbf{m} - \lambda\mathbf{f} = 0. \tag{2}$$

where $\mathbf{m} = \{m_1, \ldots, m_{nb}\}^t$, $\mathbf{f} = \{f_1, \ldots, f_{nj}\}^t$ and λ is the non-zero load factor.

Under isotropic conditions, all the moments/unit length will be bounded by the constant plastic moments of resistance/unit length in positive and negative bending, m^+ and m^-, respectively, such that:

$$\mathbf{u}m^- \ (= \bar{\mathbf{m}}) \leqslant \mathbf{m} \leqslant \mathbf{u}m^+ (= \bar{\bar{\mathbf{m}}}) \tag{3}$$

where $\mathbf{u} = \{1, \ldots, 1\}^t$ is the unit vector.

The lower bound restrictions on the moment values, $\bar{\mathbf{m}}$ are conventionally treated by a change of moment variable to $\mathbf{m} - \bar{\mathbf{m}}$ which results in eqns (2) and (3) becoming:

$$\mathbf{C}\mathbf{m}^* - \lambda\mathbf{f} = -\mathbf{C}\bar{\mathbf{m}} = \mathbf{r} \tag{4}$$

and

$$\mathbf{0} \leqslant \mathbf{m}^* \leqslant \tilde{\mathbf{m}} \quad \text{where} \quad \mathbf{m}^* = \mathbf{m} - \bar{\mathbf{m}} \quad \text{and} \quad \tilde{\mathbf{m}} = \bar{\bar{\mathbf{m}}} - \bar{\mathbf{m}}. \tag{5}$$

Equations (4) and (5) represent the conditions of equilibrium and yield, respectively, for the slab. By the lower bound theorem of plasticity, the collapse solution may therefore be obtained by maximizing the load factor, λ, subject to the linear conditions expressed by the above equations. For this to be accomplished by standard linear programming techniques [see Garvin (1960)], it is necessary that a feasible set of moments $\mathbf{m}^*$ is available which satisfies eqns (4) and (5). In general a set of feasible moments will not be known *a priori* and it is necessary to augment eqn (4) by a set of non-zero artificial variables, $\mathbf{a}$, which will

be driven to zero by the minimization process and so preserve, eventually, the original form of eqn (4). With the addition of the artificial variables, eqn (4) becomes:

$$\mathbf{a} + \mathbf{C}\mathbf{m}^* - \lambda\mathbf{f} = \mathbf{r}. \tag{6}$$

The non-negativity of the artificial variables, $\mathbf{a}$, at lower bound (zero) $\mathbf{m}^*$ and λ values, may be assured by the multiplication by -1 of any row of eqn (4) for which the relevant $\mathbf{r}$ coefficient is negative. An initial feasible solution is thereby available. To ensure that the artificial variables are driven to zero by the linear programming procedure, artificially high objective function coefficients are allocated to these variables. Taking these values to be, arbitrarily, 10^3, the programming problem becomes to minimize the objective function, z, subject to the equality constraints of eqn (6), where:

$$z = 10^3\mathbf{u}^t\mathbf{a} - \lambda \tag{7}$$

with

$$\mathbf{0} \leqslant \mathbf{a} \quad \text{and} \quad \mathbf{0} \leqslant \mathbf{m}^* \leqslant \bar{\mathbf{m}}. \tag{8}$$

In eqn (7), the negative λ coefficient is to ensure that the linear programming minimization procedure actually maximizes the load factor, whilst the upper bounds on the variables $\mathbf{m}^*$ may be dealt with implicitly [see Garvin (1960)] during the minimization.

Displacement and rotation solution

The linear programming solution will provide the collapse load factor and the boundary moment values at collapse. To obtain the yield-line pattern at collapse, it is necessary to determine the rotations along the specified boundaries, since only boundaries with non-zero rotations will represent yield-lines. Boundary rotations θ and nodal displacements $\mathbf{w}$ may be perhaps most easily determined by application of the "dual" properties of linear programming [see Munro and Da Fonseca (1978); Garvin (1960)]. With the formulation described above, the artificial variables, $\mathbf{a}$, are dual to the normal nodal displacements and the edge moment variables, $\mathbf{m}^*$, are dual to the boundary rotations. The dual properties of linear programming ensure that the objective function values at termination represent the values of the relevant dual variables. The normal displacements, $\mathbf{w}$, are therefore proportional to the objective function values (less their original values of 10^3) corresponding to the artificial variables. Similarly, the rotations about the boundary lines are proportional to the objective function values associated with the relevant edge moment variables. Rotation, and hence yield, will thus have occurred only along edges whose moment variables are associated with a non-zero objective function values.

Isotropic slabs with geometric optimization

If variation in yield-line geometry is considered, then eqn (6) becomes non-linear since both $\mathbf{C}$ and $\mathbf{f}$ are geometry dependent. The technique of sequential linear programming relies on an iterative process in which linearized approximations are used in any particular iteration. Equation (6) may be linearized by replacing each term by its first-order Taylor series approximation to give:

$$\mathbf{a} + \dot{\mathbf{C}}\mathbf{m}^* + (\dot{\mathbf{J}}_{C\mathbf{x}} - \lambda\dot{\mathbf{J}}_{f\mathbf{x}})\Delta_{\mathbf{x}} - \lambda\dot{\mathbf{f}} = \dot{\mathbf{r}}, \tag{9}$$

where $\Delta_{\mathbf{x}} = \mathbf{x} - \dot{\mathbf{x}}$ and $\mathbf{x}$ is the geometric variable vector.

In eqn (9), an overdot indicates evaluation with respect to the current geometry, and such terms therefore remain constant during the succeeding iteration. The Jacobian matrices $\dot{\mathbf{J}}_{C\mathbf{x}}$ and $\dot{\mathbf{J}}_{f\mathbf{x}}$ represent the effects of geometric variation on the equilibrium matrix, $\mathbf{C}$, and the loading vector, $\mathbf{f}$, respectively, and details of the formation of these matrices have been given previously by Johnson (1995).

The previous equilibrium constraints, eqn (6), are replaced by eqn (9) and the linear programming solution is repeated. At the conclusion of the programming procedure, the

objective function values corresponding to the geometric variables, Δ_x, will indicate the sense in which the variables need to be amended in order to modify approximately the load factor. At this stage, reductions in the load factor are sought since geometric variation represents an upper-bounded solution.

The magnitudes of the changes to the geometric variables cannot be obtained from a linear solution and must be enforced by the imposition of suitable bounds. The geometric variables are constrained by lower bounds, $\underline{\mathbf{x}}$, and upper bounds, $\bar{\mathbf{x}}$, which are designed to ensure that the confines of the slab and its basic topology are not altered. In addition, geometric variation at any iteration must be limited so that unacceptable linearization errors do not occur. If necessary, therefore, the bounds $\underline{\mathbf{x}}$ and $\bar{\mathbf{x}}$ are modified such that undue geometric distortion does not occur within any single iteration and also so as to encourage convergence. Several schemes are available for the generation of such adaptive move limits, and details of the approach adopted herein have been provided previously [see Johnson (1995)].

Orthotropic slabs without geometric optimization

If the slab is orthotropic and geometric optimization is not required, then the moment bounds $\underline{\mathbf{m}}$ and $\bar{\mathbf{m}}$ need to be calculated according to the relationship given by eqn (1), but the isotropic slab formulation may otherwise be left unchanged. If geometric optimization is required, however, it is necessary to incorporate the moment variable bounds explicitly with the equilibrium conditions and, in preparation for this development, it is convenient also to adopt such a strategy at the non-geometric optimization level. Accordingly, slack variables, $\mathbf{s}$, may be added to the upper bound constraints of eqn (5), to result in a set of equality constraints which are added to eqn (4) to give a complete set of constraints:

$$\begin{Bmatrix} \mathbf{a} \\ \mathbf{s} \end{Bmatrix} + \begin{bmatrix} \mathbf{C} \\ \mathbf{I} \end{bmatrix} \mathbf{m}^* - \lambda \mathbf{f} = \begin{Bmatrix} \mathbf{r} \\ \bar{\mathbf{m}} \end{Bmatrix} \tag{10}$$

with

$$\mathbf{0} \leqslant \mathbf{a}; \quad \mathbf{0} \leqslant \mathbf{s}; \quad \mathbf{0} \leqslant \mathbf{m}^*. \tag{11}$$

Orthotropic slabs with geometric optimization

For orthotropic slabs, the importance of treating geometric variation effects on the equilibrium and moment variable constraints simultaneously has already been established. If allowance for geometric changes is made to the moment bound conditions, eqn (3) may be expressed as:

$$\underline{\mathbf{m}} + \mathbf{J}_{\underline{m}} \boldsymbol{\Delta}_x \leqslant \mathbf{m} \leqslant \bar{\mathbf{m}} + \mathbf{J}_{\bar{m}} \boldsymbol{\Delta}_x. \tag{12}$$

In eqn (12) the Jacobian matrices, $\mathbf{J}$, represent the linearized effects of geometric change on the moment bounds and details of the construction of the matrices are provided in the Appendix. It is possible to use slack variables to convert both the lower and upper bound relationship provided by eqn (12) to equalities. This, however, results in two moment constraints for each boundary and hence doubles the number of moment constraints used in the isotropic case [eqn (10)]. For consistency, and to optimize storage, it has therefore been preferred to apply geometric variation effects to only the constraint most likely to be active for a particular edge. Thus, the constraints adopted have been:

for $\mathbf{m} \geqslant \mathbf{0}$:

$$\underline{\mathbf{m}} \leqslant \mathbf{m} \leqslant \bar{\mathbf{m}} + \mathbf{J}_{\bar{m}x} \boldsymbol{\Delta}_x \tag{13}$$

hence:

$$\mathbf{0} \leqslant \mathbf{m}^* \leqslant \tilde{\mathbf{m}}^+ + \mathbf{J}_{\bar{m}_Y} \boldsymbol{\Delta}_Y \tag{14}$$

or

$$\mathbf{s}^- + \mathbf{m}^* - \mathbf{J}_{\bar{m}_Y} \boldsymbol{\Delta}_Y = \tilde{\mathbf{m}}^+ \quad \text{with} \quad \mathbf{0} \leqslant \mathbf{s}^+; \quad \mathbf{0} \leqslant \mathbf{m}^*; \tag{15}$$

for $\mathbf{m} < \mathbf{0}$:

$$\tilde{\mathbf{m}} + \mathbf{J}_{\bar{m}_Y} \boldsymbol{\Delta}_Y \leqslant \mathbf{m} \leqslant \bar{\mathbf{m}} \tag{16}$$

hence:

$$\mathbf{0} \leqslant (\bar{\mathbf{m}} - \mathbf{m}) \leqslant \tilde{\mathbf{m}} \quad - \mathbf{J}_{\bar{m}_Y} \boldsymbol{\Delta}_Y \tag{17}$$

or

$$\mathbf{s} \quad + \mathbf{m}^{**} + \mathbf{J}_{\bar{m}_Y} \boldsymbol{\Delta}_Y = \tilde{\mathbf{m}}^-, \tag{18}$$

where $\mathbf{m}^{**} = \bar{\mathbf{m}} - \mathbf{m}$ and $\mathbf{0} \leqslant \mathbf{s}^-; \mathbf{0} \leqslant \mathbf{m}^{**}$.

With this moment constraint representation, eqn (10) takes the following form:

$$\begin{Bmatrix} \mathbf{a} \\ \mathbf{s}^+ \\ \mathbf{s}^- \end{Bmatrix} + \begin{bmatrix} \mathbf{C} & -\mathbf{C} \\ \mathbf{I} & \mathbf{0} \\ \mathbf{0} & \mathbf{I} \end{bmatrix} \begin{Bmatrix} \mathbf{m}^* \\ \mathbf{m}^{**} \end{Bmatrix} - \lambda \mathbf{f} = \begin{Bmatrix} \mathbf{r}^* \\ \tilde{\mathbf{m}}^+ \\ \tilde{\mathbf{m}}^- \end{Bmatrix} \tag{19}$$

with

$$\mathbf{0} \leqslant \mathbf{a}; \quad \mathbf{0} \leqslant \mathbf{s}^-; \quad \mathbf{0} \leqslant \mathbf{s}^+; \quad \mathbf{0} \leqslant \mathbf{m}^*; \quad \mathbf{0} \leqslant \mathbf{m}^{**}. \tag{20}$$

The objective function and the remainder of the procedure are then unchanged. Employing this modified version of orthotropy treatment results in the iteration procedure for the simple orthotropic slab considered previously coinciding with that of the affine based analysis [Fig. 2(c)]. The modified approach to orthotropy is therefore clearly much more powerful than the simplified method employed initially and the modified approach has been used to generate the solutions given to a range of examples in the next section.

EXAMPLES

In each case, the sequential linear programming technique has been used to evaluate the uniformly distributed collapse load, q_u (equal to λq). For numerical purposes, the generalized uniformly distributed load, q, the generalized length, l, and the generalized moment of resistance unit length, m, were all taken to be unity. For such values, it follows that the quoted numerical collapse load values, q_u, are equal to the relevant load factors, λ, obtained from the programming solutions.

Simply supported square slab with one free edge and skewed reinforcement

The orthotropic square slab shown in Fig. 3 is simply supported on three sides and free on the remaining side. Although still a simple geometric layout, the orthotropic

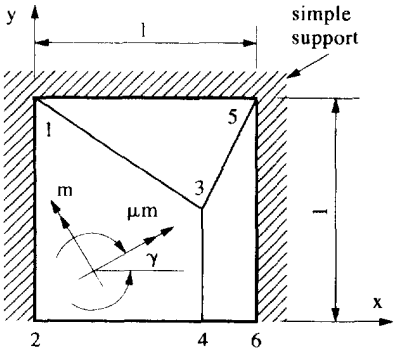

Fig. 3. Orthotropic square slab with skewed reinforcement.

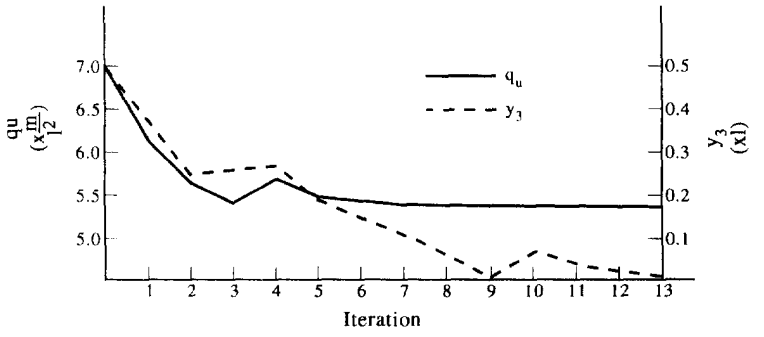

Fig. 4. Solution graph for orthotropic square slab solution.

reinforcement is skewed to the supports so that an affine transformation is not straightforward in this case. Wood (1961) has developed a closed form solution for this problem in terms of the reinforcement orientation angle, γ, and the reinforcement ratio, μ. The meshing shown in Fig. 3 has been used for a series of automated analyses, using the two geometric variables x_3 and y_3 (x_4 being constrained to equal x_3). The quadrilateral subdivisions in the mesh were divided into triangles by a pre-processor which inserts diagonals for analysis purposes.

The analyses all showed close agreement with Wood's solution and, as a possibly extreme case, results will be quoted for the γ, μ parameters of 67.5° and 0.1, respectively. Wood's solution for this case is $q_u = 5.38(m/l^2)$ with $x_3 = 0.5l$ and $y_3 = 0.02l$. The modified orthotropic automated analysis provided $q_u = 5.39(m/l^2)$ and $x_3 = 0.50l$; $y_3 = 0.01l$ after 13 iterations. By way of comparison, the simple orthotropic approach again converged after 22 iterations to an incorrect solution of $q_u = 6.50(m/l^2)$ and $x_3 = 0.49l$; $y_3 = 0.52l$.

The progress of the modified orthotropic analysis iterations is shown in Fig. 4, which illustrates several typical features of the iterative process. Reductions in load factor, for instance, generally occur more smoothly than do alterations in geometric parameters (y_3 being used as typical parameter in this case). Furthermore, major reductions in load factor are generally only achieved in the first few iterations, the remaining iterations being required to achieve the rather stringent convergence criterion used of less than 0.1% variation in load factor between successive iterations. The stringent convergence test is, however, needed if any reasonable accuracy is to be obtained for collapse mode geometry since, as featured in Fig. 4, load factors are typically insensitive to geometric variation in the vicinity of their minima.

Non-rectilinearly bounded slab with varying support conditions

The slab shown in Fig. 5(a) may be expected to be an even more demanding example since it is non-rectilinearly bounded, has varying support conditions and the isotropic negative reinforcement is skewed to the orthotropic positive reinforcement. The subdivision indicated in the figure was employed, with the quadrilateral regions again being automatically subdivided. To ensure the geometrical consistency of the expected collapse mechanism, edge 3–5 was constrained to pass through the intersection of the boundary lines of rotation 2–4 and 1–6, shown as node 7 in Fig. 5(b). The geometrical parameters were taken as y_5 and the position of node 3 along the line 7–5. The chosen initial geometry was defined by $x_3 = 2l$ and $y_5 = 2.4l$. For this geometry, the orthotropic formulation gave a load factor, $\dot{\lambda} = 0.872(m/l^2)$, which may be compared with the approximate value of $\dot{\lambda} = 0.942(m/l^2)$, calculated by Brohn (1990). Geometrical optimization converges after six iterations to $\ddot{\lambda} = 0.818(m/l^2)$ (a 6.6% decrease from the starting value). Position 5 remains largely unaffected by the optimization ($\ddot{y}_5 = 2.34l$), but position 3 retreats significantly from the fixed edge ($\ddot{x}_3 = 3.92l$).

Slab with point support

Further support variety occurs in the rectangular slab shown in Fig. 6(a), which has two adjacent free edges, two simply supported edges and an internal point support situated

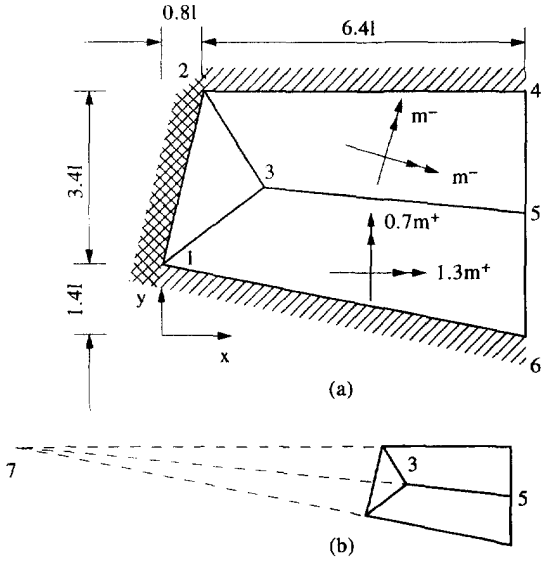

Fig. 5. Non-rectilinearly bounded slab with varying support conditions.

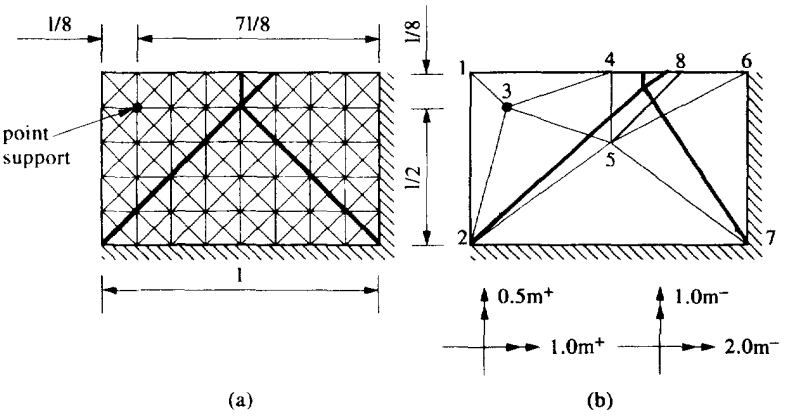

Fig. 6. Slab with point support. (a) "Fine" mesh. (b) "Simplified" mesh.

at $0.125l$ from each of the free edges. Since the collapse mode is not known *a priori* in this case, a strategy, previously recommended by Johnson (1994a), has been adopted in which a fine "finite-element" type mesh is analysed initially, without geometric optimization, in order to establish the form of the collapse mode. Following this precept, the mesh shown in Fig. 6(a) was analysed and gave a load factor $\lambda = 19.2\ (m/l^2)$, which was associated with the collapse mode shown as a yield-line pattern in Fig. 6(a) and as an isometric projection in Fig. 7.

To verify this solution and to examine the effects of geometric optimization, the simpler meshing shown in Fig. 6(b) was subsequently examined using x_5, y_5, x_4 (equal to x_5) and x_8 as the geometric variables. This mesh is capable of developing not only the mode indicated by the finite-element type meshing, but also modes involving "fan" type mechanisms around the point support. However, given the heavier negative reinforcement (typical of practical slab design involving point supports), the development of a fan system is perhaps unlikely in this case. This indeed proves to be so, and the mechanism developed is similar to that of the initial fine meshing. The load factor for the starting geometry [$\dot{x}_4$ (equal to $\dot{x}_5$) $= 0.5l$, $\dot{y}_5 = 0.5l$ and $\dot{x}_8 = 0.75l$] of the simplified mesh was $\dot{\lambda} = 20.8\ (m/l^2)$ and at the converged geometry [$\ddot{x}_4$ (equal to $\ddot{x}_5$) $= 0.619l$, $\ddot{y}_5 = 0.572l$ and $\ddot{x}_8 = 0.696l$] the load factor had reduced to $\ddot{\lambda} = 18.5\ (m/l^2)$. This final load factor was achieved after 18 iterations and represents a 4% decrease from the fine mesh solution. Such modest load factor reductions provided by

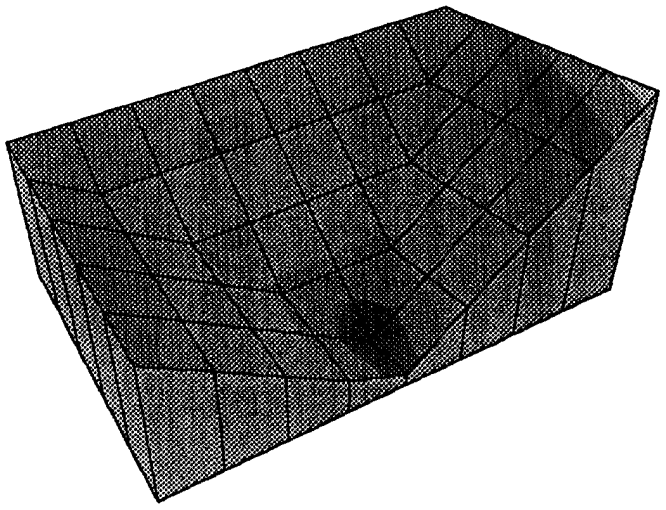

Fig. 7. Collapse mode for slab with point support.

the geometrical optimization of simplified meshes have been found previously [see Johnson (1994b)] to be typical of most situations other than mechanisms involving fan systems.

CONCLUSIONS

(1) It is not effective to rely on between iteration modification to represent the effects of geometric variation on ultimate yield-line moment values in orthotropic slabs. Such a strategy leads to an unpredictable formulation which may converge slowly, may diverge or may converge to an erroneous solution.

(2) If linearized yield-line ultimate moment sensitivities are included within the geometric iterations, then an effective formulation results, which has been shown to converge satisfactorily for a range of support and geometrical slab layout conditions.

(3) Incorporation of ultimate moment sensitivities within the geometric iterations leads to an increased number of constraints since ultimate moment constraints need to be treated explicitly, rather than by an upper and lower bound treatment. The number of additional constraints may be halved by only including the effects of geometrical variation on the ultimate moment constraint for the nature of moment most likely to be active at any given iteration.

(4) As experienced previously for the isotropic slabs (Johnson, 1994a), load factors for orthotropic slabs, in the region of the minimum factor, are rather insensitive to geometric yield-line variation. It follows that collapse pattern layouts are likely to be determined to a lower degree of accuracy than ultimate loads and that a close convergence tolerance for the minimum load factor is required if geometrical accuracy is of importance.

REFERENCES

Brohn, D. (1990). *Understanding Structural Analysis*. BSP Professional Books, Oxford.
Garvin, W. W. (1960). *Introduction to Linear Programming*. McGraw-Hill, New York.
Johnson, D. (1994a). Mechanism determination by automated yield-line analysis. *Struct. Engr* **72**, 323–327.
Johnson, D. (1994b). Automated yield-line analysis of beam-slab systems. Submitted to *Struct. Engng Mech.*
Johnson, D. (1995). Yield-line analysis by sequential linear programming. *Int. J. Solids Structures*. **32**(10), 1395–1404.
Munro, J. and Da Fonseca, A. M. A. (1978). Yield-line method by finite elements and linear programming. *Struct. Engr* **56B**, 37–44.
Wood, R. H. (1961). *Plastic and Elastic Design of Slabs and Plates*. Thames and Hudson, London.

APPENDIX: JACOBIAN MATRICES

Formation of $\mathbf{J}_{\bar{m}x}$ *and* $\mathbf{J}_{\bar{\bar{m}}x}$

By definition:

$$\mathbf{J}_{mx} = \left\{ \cdots, \frac{\partial m}{\partial x_i}, \cdots \right\}^t, \tag{A1}$$

where m is either $\bar{m}$ or $\bar{\bar{m}}$ and x_i is a geometric variable.

To examine the variation of m with x_i recall that, by the Johansen yield condition [eqn (1) and Fig. 1],

$$m = m_u \cos^2 \alpha + m_l \sin^2 \alpha. \tag{A2}$$

Hence:

$$\frac{\partial m}{\partial x_i} = 2\left[m_u \cos\alpha \frac{\partial \cos\alpha}{\partial x_i} + m_l \sin\alpha \frac{\partial \sin\alpha}{\partial x_i} \right]; \tag{A3}$$

but $\alpha = \theta - \phi$ (Fig. 1), hence:

$$\frac{\partial m}{\partial x_i} = 2\left[m_u \cos\alpha \frac{\partial(\cos\theta\cos\phi + \sin\theta\sin\phi)}{\partial x_i} + m_l \frac{\partial(\sin\theta\cos\phi - \cos\theta\sin\phi)}{\partial x_i} \right]; \tag{A4}$$

and

$$\frac{\partial m}{\partial x_i} = 2\left[(m_u \cos\alpha\cos\phi - m_l \sin\alpha\sin\phi) \frac{\partial\cos\theta}{\partial x_i} \right] + 2\left[(m_u \cos\alpha\sin\phi + m_l \sin\alpha\cos\phi) \frac{\partial\sin\theta}{\partial x_i} \right]. \tag{A5}$$

If the yield-line segment is defined by end nodes 1 and 2 (Fig. A1), having coordinates (x_1, y_1) and (x_2, y_2) then in eqn (A1), all terms are zero for which $x_i \neq x_1, y_1, x_2$ or y_2. If $x_i = x_1, y_1, x_2$ or y_2, then the derivatives required by eqn (A5) may be shown to be:

$$\frac{\partial\cos\theta}{\partial x_1} = -\frac{Y^2}{L^3}; \quad \frac{\partial\cos\theta}{\partial x_2} = \frac{Y^2}{L^3}; \quad \frac{\partial\cos\theta}{\partial y_1} = \frac{XY}{L^3}; \quad \frac{\partial\cos\theta}{\partial y_2} = -\frac{XY}{L^3} \tag{A6}$$

and

$$\frac{\partial\sin\theta}{\partial x_1} = \frac{XY}{L^3}; \quad \frac{\partial\sin\theta}{\partial x_2} = -\frac{XY}{L^3}; \quad \frac{\partial\sin\theta}{\partial y_1} = -\frac{X^2}{L^3}; \quad \frac{\partial\sin\theta}{\partial y_2} = \frac{X^2}{L^3}. \tag{A7}$$

In eqns (A6) and (A7), X and Y are the projections of the yield-line segment on the respective coordinate axes and L is the length of the segment (Fig. A1).

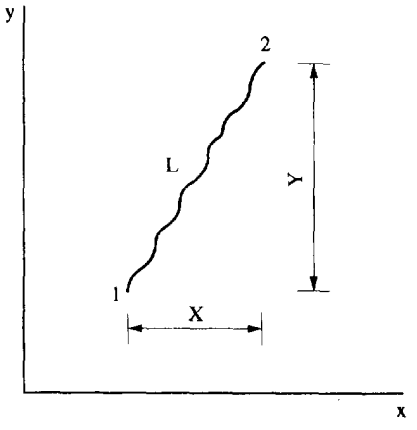

Fig. A1. Yield-line segment.